

## Production and identification of flux-pinning defects by electron irradiation in $\text{YBa}_2\text{Cu}_3\text{O}_{7-x}$ single crystals

J. Giapintzakis, W. C. Lee, J. P. Rice, D. M. Ginsberg, and I. M. Robertson

*Department of Physics and Materials Research Laboratory, University of Illinois at Urbana-Champaign,  
1110 West Green Street, Urbana, Illinois 61801*

R. Wheeler and M. A. Kirk

*Materials Science Division, Argonne National Laboratory, Argonne, Illinois 60439*

M.-O. Ruault

*Centre de Spectrométrie Nucléaire et de Spectrométrie de Masse, Orsay, France*

(Received 19 December 1991)

An enhancement in  $J_c$  of  $\text{YBa}_2\text{Cu}_3\text{O}_{7-x}$  single crystals in a magnetic field is observed after irradiation with 1-MeV electrons. Typically, a factor-of-2 increase in  $J_c$  is deduced from magnetic hysteresis loops at 10 K and 1 T with  $\mathbf{H} \parallel \mathbf{c}$ . This enhancement is about  $\frac{1}{2}$  of that produced by proton and neutron irradiations under similar measurement conditions. *In situ* transmission-electron-microscopy studies found no visible defects induced by electron irradiation, which means that point defects or small clusters (of size  $< 2$  nm) are responsible for the extra pinning. Annealing studies suggest that effective pinning centers for  $\mathbf{H} \parallel \mathbf{c}$  do not include oxygen vacancies in the Cu-O chains. Based on calculations of cross sections for displacements on the different sublattices, and in conjunction with the results of a  $J_c$  calculation by Kes, we suggest that the most likely pinning defect is the displacement of a Cu atom from the  $\text{CuO}_2$ -plane sites.

### I. INTRODUCTION

The discovery of the high-temperature superconductors (HTS's) has led to many speculations about superconducting applications at liquid-nitrogen temperature. However, in addition to a high critical temperature  $T_c$  and large upper critical field, a large critical-current density  $J_c$  is required for certain applications. In this regard experiments involving irradiation of HTS's with various energetic particles such as neutrons,<sup>1,2</sup> protons,<sup>3</sup> and electrons<sup>4,5</sup> have been performed. However, many studies have concentrated only on increasing  $J_c$  rather than on fundamental investigations of flux pinning.

Electron irradiation is an appropriate method to study the effect of certain lattice defects on superconducting properties because by varying the electron energy we can selectively produce defects on the different sublattices. These defects are randomly distributed in space. Shiraishi, Kato, and Kuniya<sup>4</sup> sequentially irradiated Y-Ba-Cu-O sintered pellet with 3-MeV electrons up to  $2.25 \times 10^{18} \text{ cm}^{-2}$  at about 370 K and carried out  $M(H)$  measurements at 77 K in fields up to 1 T. They observed a maximum enhancement of 53% at 1 T by electron irradiation to a dose of  $1.75 \times 10^{18} \text{ cm}^{-2}$  and then a decrease upon further irradiation. Konczykowski<sup>5</sup> investigated the screening effect of a Y-Ba-Cu-O single crystal as a function of damage produced by 2.5-MeV electrons at low temperatures with a short annealing period at room temperature. He observed an enhancement of screening efficiency, from which he concluded that the defects induced by electron irradiation increased the pinning force

of the flux vortices and hence  $J_c$ . Distinguishing between the effect of an increased number of pinning centers and the creation of more efficient centers was not possible.

Civale *et al.*<sup>3</sup> irradiated several Y-Ba-Cu-O single crystals with 3-MeV protons at room temperature and measured  $M(H)$  curves at 5 and 77 K in fields up to 5.5 T. They observed large enhancements of  $J_c$  at 1 T, ranging between 4–10 times the preirradiation  $J_c$  value ( $J_{c0}$ ) at 5 K and between 10–100 times  $J_{c0}$  at 77 K. Transmission-electron-microscopy (TEM) studies showed the presence of isolated defect clusters after irradiation. However, based on an analysis of “ $J_c$  scaling,” they concluded that the dominant pinning sites were not these clusters, but randomly distributed point defects generated by the protons.

The aim of this work is (a) to study systematically the effects of 1-MeV electron irradiation upon the superconducting properties, such as  $T_c$  and  $J_c$ , of high-quality Y-Ba-Cu-O single crystals, (b) to understand the effect of defects in the sublattices of oxygen and the other cations on the magnetic flux pinning, and (c) to explain the observed difference in the  $J_c$  enhancement produced by 1-MeV electron and 3-MeV proton irradiations.

### II. EXPERIMENTAL PROCEDURE

#### A. Sample preparation

The measurements were performed on single crystals of Y-Ba-Cu-O that were grown by a “self-flux” method from nonstoichiometric  $([\text{Y}]:[\text{Ba}]:[\text{Cu}])$  ratios of 1:4:10

TABLE I. Characteristics of the samples used in this study.

Crystal	$J_{c0}$ 10 K, 1 T (A cm <sup>-2</sup> )	$J_{c0}$ (40 K, 1 T) (A cm <sup>-2</sup> )	Dose rate $\Phi$ [e/(cm <sup>2</sup> sec)]	$T_{\text{irrad}}$ (K)	$T_{\text{ann}}$ (K)
<i>A</i> twinned	$1.25 \times 10^6$	$1.88 \times 10^5$	$2.79 \times 10^{15}$	300	
<i>B</i> twinned			$2.50 \times 10^{15}$	300	
<i>C</i> untwinned			$1.77 \times 10^{15}$	300	
<i>D</i> untwinned	$1.64 \times 10^6$	$9.9 \times 10^4$	$1.61 \times 10^{15}$	300	
<i>E</i> twinned	$1 \times 10^6$	$2.5 \times 10^4$	$1.52 \times 10^{15}$	100	300
<i>F</i> twinned			$6.66 \times 10^{15}$	300	473

melts in Y<sub>2</sub>O<sub>3</sub>-stabilized ZrO<sub>2</sub> crucibles.<sup>6</sup> Crystallization occurred during a slow cooling (2 °C/h) of the melt in air from 1000 to 865 °C. The as-grown crystals were air quenched from 865 °C to room temperature and then mechanically extracted from the matrix. The crystals were small-sized platelets with typical dimensions of 2 × 1.5 × 0.1 mm<sup>3</sup>, with the smallest dimension in the *c* direction. Selected crystals were annealed in oxygen at 650 °C for 1 h and then at 450 °C for several days while situated on a fully oxygenated Y-Ba-Cu-O sintered pellet. This procedure yielded high-quality samples, and some were free of twinning over more than 90% of their area, as determined by observation of the remaining twinning under polarized light. The samples used in this study (see Table I) included twinned and untwinned crystals, and they were cleaved to a nearly square shape with dimensions up to 0.5 × 0.5 mm<sup>2</sup> and thickness of 10–60 μm. The small size of the samples was necessary to minimize the time of irradiation with a limited irradiating current. The cleaved samples were reannealed to relieve the strains introduced by the cleaving process. The transition temperatures  $T_c$  of the annealed crystals were in the range 90–91 K with a transition width of approximately 2 K. Preirradiation  $J_c$  values in a magnetic field of 1 T at 10 and 40 K were approximately  $1 \times 10^6$  and  $1 \times 10^5$  A/cm<sup>2</sup>, respectively, for  $\mathbf{H} \parallel c$  axis.

### B. Magnetic measurements

The magnetic properties of the samples before and after each electron irradiation were measured in a Quantum Design superconducting quantum interference device (SQUID) magnetometer. In order to minimize the background contribution to the measured magnetic moment, we used as a sample holder a symmetric high-purity quartz tube. The tube was attached to the sample rod of the magnetometer by a string so that it would be held parallel to the direction of the magnetic field by the action of gravity. The sample was embedded in an incision in the middle part of the tube between two smooth very small pieces of weighing paper to avoid friction with the rough surface of the quartz tube. Finally, the sample

and paper were kept in place by wrapping two turns of Teflon tape around them.

The  $T_c$  was determined from the temperature dependence of the magnetic shielding curve. The transition curves were obtained by cooling the sample in zero field to 5 K, applying a constant field of 10–25 Oe, and measuring the magnetization with increasing temperature.

The field dependence of the magnetization  $M(H)$  was measured at 10 and 40 K for fields along the *c* direction and varying *H* from 0 to 4 T. The  $M(H)$  measurements were done in the “no-overshoot” magnet mode, and the data at each field were taken 5 min after the field change. This delay was used to stabilize the SQUID magnetometer and so that the magnetization inside the sample had enough time to relax to a relatively stabilized value. We found it necessary to use scan length of less than 4 cm to ensure field uniformity of better than 0.19%.

The demagnetizing factors for the samples were calculated, using the ellipsoidal approximation, to be between 0.85 and 0.97. However, no attempt was made to correct the  $M(H)$  data, since we were interested only in the relative changes of the  $J_c$  in this study.

### C. Electron irradiation

The high-voltage electron microscope (HVEM) accelerator facility at Argonne National Laboratory was used for all the electron irradiations. One of the advantages of this facility is that it allows *in situ* TEM imaging and diffraction between 100 keV and 1.1 MeV to be performed on samples held at temperatures between 10 K and 1000 °C. When we operated the HVEM as a source of electrons for the irradiations, we used the low-magnification mode to spread the beam sufficiently to irradiate uniformly crystals with cross sections up to 0.75 × 0.75 mm<sup>2</sup>. The dosimetry was performed by measuring the total beam current entering a removable Faraday cup that was inserted just above the sample. The beam area irradiating the crystal was measured by film exposure. The absolute accuracy of the dosimetry was close to 10%. Much effort was expended to ensure that the temperature of the sample did not exceed a nom-

inal value of 300 K. This was accomplished by rigidly mounting the bulk crystal on the high-mesh face of a  $100 \times 300$  mesh folding copper grid with silver paint. The 3-mm grid was then clamped with a spring-type ring to the sample holder of a single-tilt sample stage that was used as a heat sink. Before we perfected the above procedure, excessive beam heating of the samples was observed by measuring unusual  $T_c$  and  $J_c$  changes following irradiations. The crystals were demounted for magnetization work by using 2-butoxyethyl acetate without affecting the quality of the surface or the sample's bulk properties.

The irradiations were performed with 1-MeV electrons in a vacuum of  $10^{-6}$  Torr at 100 and 300 K. The dose rate  $\Phi$  was kept to the minimum practical value for reasonable irradiation times. The flat crystals were irradiated  $8^\circ$ – $10^\circ$  off the  $c$  axis to avoid electron channeling. The maximum dose was  $7 \times 10^{19} \text{ cm}^{-2}$ .

#### D. TEM

In addition to the electron irradiation of bulk single crystals, the HVEM was employed to study *in situ* the defect microstructure produced in thin samples under various electron-irradiation conditions, including those used to produce pinning defects in the bulk crystals. Bulk single crystals of Y-Ba-Cu-O were made thin by being electropolished<sup>7</sup> and were irradiated with 1-MeV electrons to doses ranging from  $10^{18}$  to  $10^{20} \text{ cm}^{-2}$  and at dose rates from  $10^{15}$  to  $10^{18} \text{ cm}^{-2} \text{ sec}^{-1}$ . *In situ* imaging conditions in the HVEM employed diffraction contrast using a  $G=200$  dark field at electron voltages of both 1 MeV and 100 keV (below the threshold for atomic displacements).

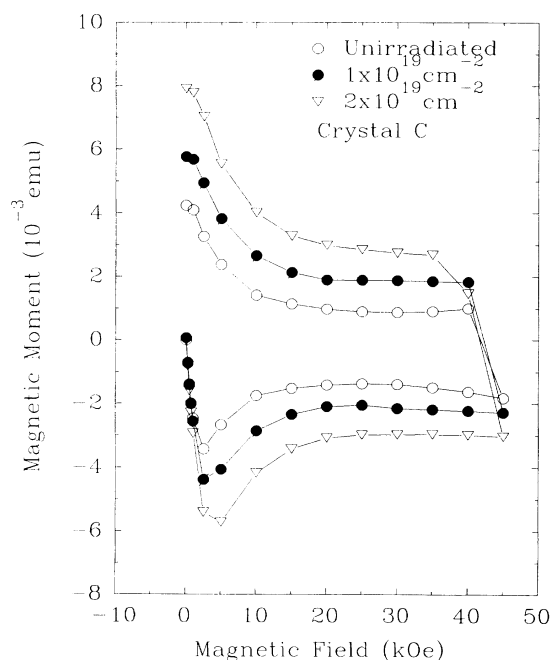


FIG. 1. Magnetic moment as a function of applied magnetic field for crystal C at various doses of electron irradiation, at 10 K.

### III. RESULTS

#### A. $J_c$

The  $M(H)$  curves at  $T=10$  K for crystal C, irradiated to doses of  $1 \times 10^{19}$  and  $2 \times 10^{19} \text{ cm}^{-2}$  at 300 K, are illustrated in Fig. 1, in comparison with a curve obtained for the sample in the unirradiated condition. The figure clearly indicates an increase of the width of the hysteresis loop ( $\Delta M$ ) following irradiation. According to the critical-state Bean model,<sup>8</sup>  $J_c \propto \Delta M$ , where  $\Delta M$  is the difference between the upper and lower branches of the  $M(H)$  loop. Hence  $J_c$  has been enhanced as a consequence of the extra pinning generated by the irradiation-induced defects.

The unchanged slope of the initial part of the virgin magnetization curve in Fig. 1 indicates that the amount of the superconducting material is not significantly reduced at these doses of irradiation.

The ratio of the  $J_c$  in the irradiated state to the preirradiation value  $J_{c0}$  at  $H=1$  T as a function of fluence is shown in Fig. 2 for crystals A, B, C, and D. To avoid the complication introduced by the large-time relaxation of  $M(H)$  in these materials, we have concentrated on results at low temperature,  $T=10$  K, where those effects are minimum. While there is a distribution of values of  $J_c/J_{c0}$  from crystal to crystal, the trends with dose are the same. First, there is a rise in reduced  $J_c$ , followed by a saturation and an eventual decrease with higher doses. A closer look at the first stage for crystals C and D reveals the existence of a small peak or shoulder at a dose of  $(6-8) \times 10^{17} \text{ cm}^{-2}$ . The optimum value of the reduced  $J_c$ , at  $T=10$  K and  $H=1$  T for crystal C, is 2.6, occurring at doses on the order of  $2 \times 10^{19} \text{ cm}^{-2}$ .

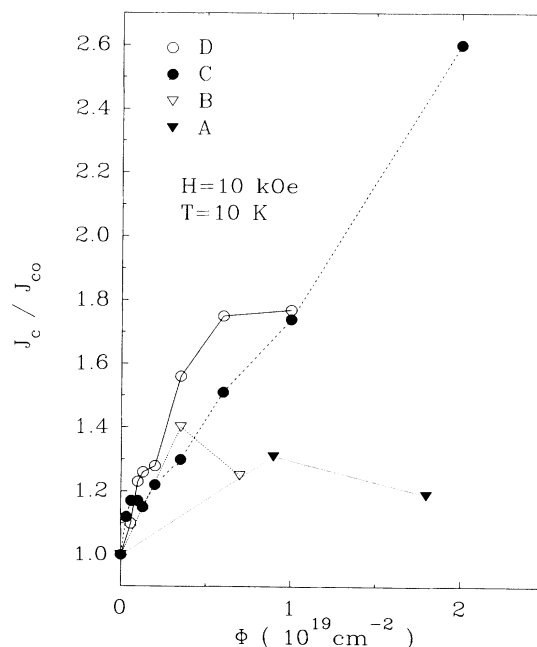


FIG. 2. Reduced critical-current density ( $J_c/J_{c0}$ ) at  $H=1$  T as a function of irradiation dose at 10 K for several of the crystals measured.

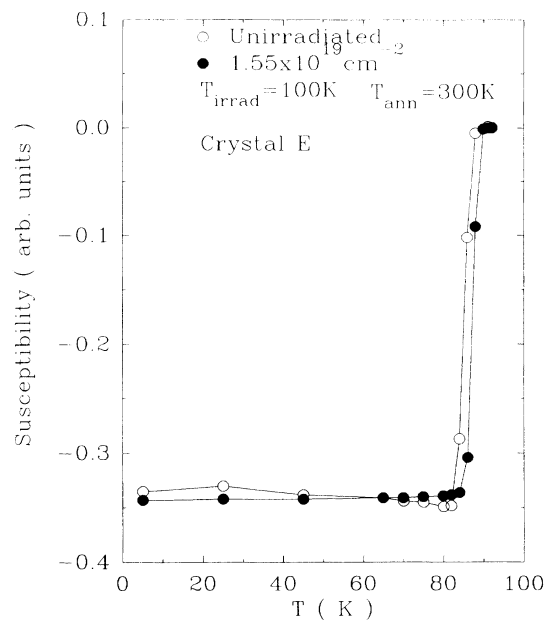


FIG. 3. Susceptibility as a function of temperature for crystal *E*: in the unirradiated state ( $\circ$ ) and following electron irradiation at 100 K with a subsequent annealing at 300 K for a few days ( $\bullet$ ).

#### B. Annealing studies

Crystal *E* was irradiated to a dose to  $1.55 \times 10^{19} \text{ cm}^{-2}$  at 100 K and then annealed at 300 K over a period of a few days before we measure its  $T_c$  and  $M(H)$  curves. We

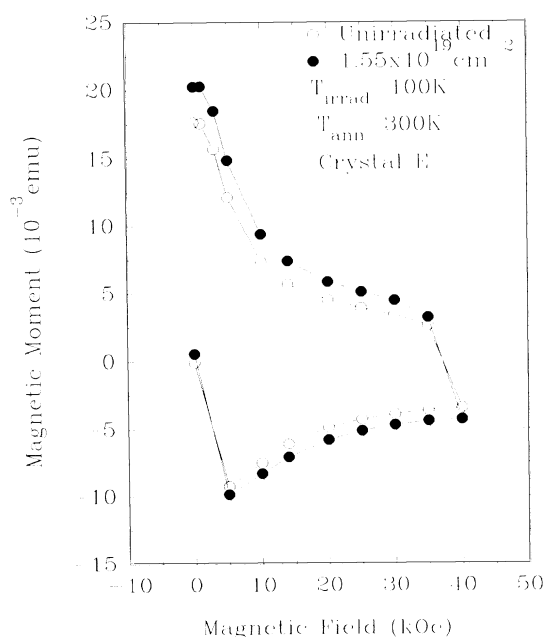


FIG. 4. Magnetic moment as a function of applied magnetic field at 10 K for crystal *E*: in the unirradiated state ( $\circ$ ) and after electron irradiation at 100 K followed by annealing at 300 K for a few days ( $\bullet$ ).

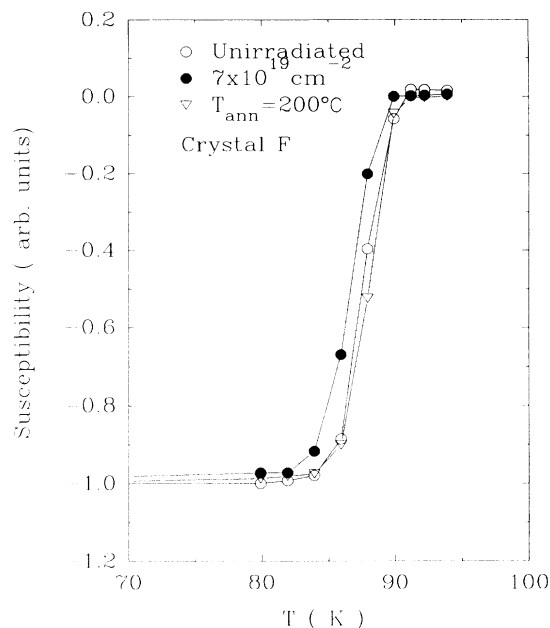


FIG. 5. Susceptibility as a function of temperature for crystal *F*: in the unirradiated state ( $\circ$ ), after electron irradiation at 300 K ( $\bullet$ ), and after annealing the irradiated crystal for 4 h at 200°C in a 100%-dried oxygen atmosphere ( $\nabla$ ).

observed, as shown in Figs. 3 and 4, an increase of  $T_c$  by about a degree, as well as an enhancement of the  $J_c$  by 22%.

After we irradiated crystal *F* to a dose of  $7 \times 10^{19} \text{ cm}^{-2}$

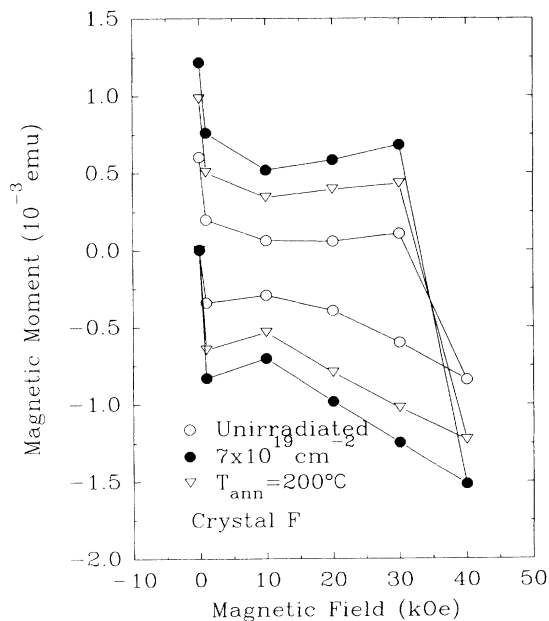


FIG. 6. Magnetic moment as a function of applied magnetic field at 40 K for crystal *F*: in the unirradiated state ( $\circ$ ), after electron irradiation at 300 K ( $\bullet$ ), and after annealing the irradiated crystal for 4 h at 200°C in a 100%-dried oxygen atmosphere ( $\nabla$ ).

### 1.1-MeV Electron Irradiation to $3 \times 10^{20} \text{ cm}^{-2}$

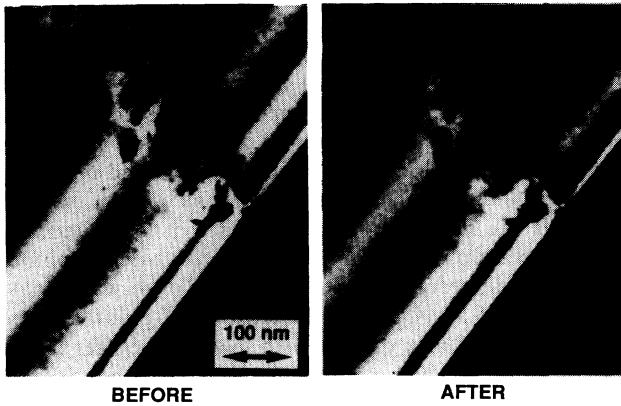


FIG. 7. TEM micrographs of the same region (a) before and (b) after electron irradiation ( $G = 200$  dark field).

at 300 K, it exhibited an observable decrease of  $T_c$ , but an enhancement of  $J_c$ . (This sample showed the highest  $J_c$  enhancement of all the samples we have studied.  $J_c/J_{c0} = 3$  at  $T = 10$  K and  $H = 1$  T.) Then it was annealed in a 100%-dried oxygen atmosphere at 200 °C for 4 h. Figures 5 and 6 show that during annealing we recovered 100% of  $T_c$ , but only about 25% of  $J_c$ .

#### C. TEM

Figure 7 illustrates that no defect structure could be observed in the *in situ* HVEM experiments under electron-irradiation conditions similar to those of the bulk-crystal irradiations. The same was observed under other irradiations up to higher doses and employing higher dose rates. The higher doses and dose rates can compensate for the loss of mobile defects to nearby surfaces in the thinned TEM samples, thereby achieving a defect structure similar to the bulk-crystal irradiations. Under the HVEM imaging conditions employed, the resolution limit was  $\leq 2$  nm. No defect structure larger than this resolution limit was observed.

### IV. DISCUSSION

#### A. Irradiation

The data contain information on the effects of displacement damage upon superconducting properties, such as magnetic-flux pinning and  $T_c$ , produced by irradiation of Y-Ba-Cu-O single crystals with 1-MeV electrons. During irradiation, the incident electrons collide with the target Y, Ba, Cu, and O atoms, transferring part of their energy, producing primary knock-on atoms (PKA's). These PKA's in turn are able to produce defects if their energy exceeds the threshold for producing a stable displaced atom. The primary defect is thus usually considered to be a vacancy-interstitial atom pair, although variations on this simple concept should be considered in a complex structure. The final stable defect structure might also

consist of clusters of point defects if either the vacancy or interstitial is mobile at the irradiation temperature. Depending on the defect's location within the unit cell as well as the size and concentration of the point or small cluster defects, the superconducting properties of the material can be altered, possibly increasing  $J_c$ , if these defects can effectively pin magnetic-flux vortices by locally depressing the superconducting order parameter.

In conventional superconductors the flux-pinning effect of defects induced by electron irradiation is relatively weak. This has been attributed to the small spatial extent of the point defects with respect to the large coherence length, which is thought to scale the vortex-defect interaction.<sup>9</sup> In Y-Ba-Cu-O the coherence lengths are  $\xi_c(0) \approx 3$  Å and  $\xi_{ab} \approx 16$  Å,<sup>16</sup> so we expect the point defects or small clusters possibly to be efficient pinning centers.

Making the simple assumption that it requires about 20 eV to permanently displace any of the four atom types, this threshold is exceeded by 1-MeV electrons for all atoms, as illustrated in Fig. 8. From this figure, which is based on the simple relativistic kinematic relation for electron-atom scattering,<sup>10</sup> it is found that the minimum electron energies required for displacement are 129, 413, 532, and 730 keV for O, Cu, Y, and Ba, respectively, assuming a threshold of 20 eV recoil energy.

According to Katz and Penfold's empirical range-energy relation,<sup>11</sup> 1-MeV electrons have a range of 646  $\mu\text{m}$  in Y-Ba-Cu-O, which far exceeds our crystal thicknesses of 10–60  $\mu\text{m}$ . The calculated energy loss for electrons at 1 MeV is about 1.4 keV/ $\mu\text{m}$ , which yields an average energy loss of 2.8–8.4 % for these crystal thicknesses. Thus the 1-MeV electrons lose little energy passing through the crystal and easily exceed the threshold energy needed to displace even the heaviest atom, Ba, throughout the entire crystal thickness.

At 1-MeV electron energy, the cross sections for displacing the four atom types range from about 15 to 50 b, again assuming the 20-eV displacement threshold. This yields a mean free path between displacement events caused by a single electron to greatly exceed the crystal

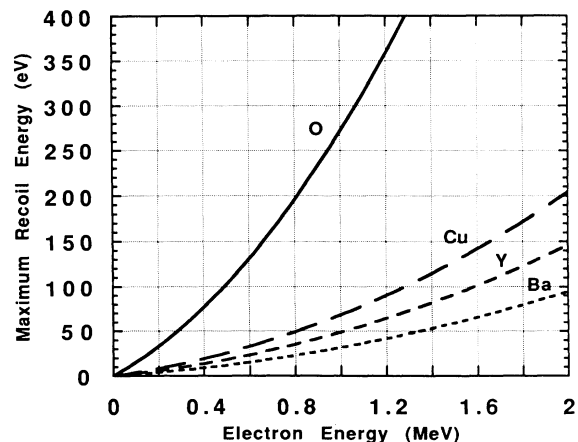


FIG. 8. Maximum recoil energies for electron irradiation up to a maximum incident energy of 2 MeV.

thickness. Thus, in a thin crystal (10–60  $\mu\text{m}$ ), roughly 1 in a 1000 incident electrons produces a recoil exceeding the threshold energy for defect formation, and these defects are randomly dispersed through the crystal thickness.

### B. $J_c$ enhancement

Based on calculations of cross sections for the different sublattices, using threshold energies near a recently determined electron-energy threshold for producing pinning (400–600 keV),<sup>17</sup> a reasonable suggestion for the primary pinning defect can be made. With a threshold for displacement of 20–30 eV and a consequent cross section for displacement of 20–50 b, the most likely pinning defect appears to be the displacement of a copper atom from the  $\text{CuO}_2$ -plane sites. A vacant Cu site would certainly produce a strong disruption of the local electronic structure in the strongly superconducting planes. A cross section of 20–50 b is large enough to account for a copper-vacancy concentration on the planes at an electron dose near  $1 \times 10^{19} \text{ cm}^{-2}$ , consistent with a calculation by Kes<sup>12</sup> for pinning by point defects for our measured  $J_c$  (although Kes assumes this defect to be an oxygen vacancy). The electron threshold energy of 400–600 keV would imply an oxygen threshold energy of about 100 eV, if this were to be the pinning defect. The consequent oxygen cross section for displacement would then be only about 2 b, resulting in an oxygen-vacancy concentration at the same electron dose far too low to explain our observed flux pinning, according to the Kes calculation.

The first smaller peak or shoulder in the dose curve is then most likely explained by defects in the Y plane produced by either Y displacement or Ba displacement into this plane. The cross section for this event is of order 5 times greater than Cu displacement, if the relevant thresholds on Y and Ba are 15–20 eV, a reasonable range. Defects on the Y plane might be expected to produce flux pinning by local-strain effects, but it is not unreasonable to suggest that these pinning defects would be weaker than those of Cu vacancies on the neighboring  $\text{CuO}_2$  planes.

An interesting question that is raised by looking at the dose curves for crystals *A* and *B* is, why does the reduced  $J_c$  decrease beyond a certain dose? For the conventional superconductors a decrease was associated either with the overlap of the defects<sup>13</sup> or the degradation of the thermodynamic superconducting properties,<sup>14</sup> such as  $T_c$  and  $H_{c2}$ . Assuming that each Cu recoil event creates a point-defect pinner, we calculated that the mean lateral distance ( $\parallel ab$  plane) between the pinning centers would be approximately 46 Å for a dose of  $1 \times 10^{19} \text{ cm}^{-2}$ . Since  $\xi_{ab} \sim 15 \text{ Å}$  at 10 K, this would suggest that the “overlap” dose is in the range of low  $10^{19}$  per  $\text{cm}^2$ . In addition, as  $\xi_{ab}$  becomes greater with increasing temperature, this would in part explain why the peak of maximum enhancement occurs at lower doses for higher temperatures.<sup>3,4</sup>

The observed variation in the dose dependence of  $J_c/J_{c0}$  from crystal to crystal can be explained by the fact

that each crystal has a different preirradiation defect state. The irradiation-induced point defects react with the preirradiation defects and change them. Also, the mobility of the created point defects depends on the “quality” of the crystal and temperature of the irradiation. If we assume that a small Cu cluster defect is a stronger pinner than a Cu point defect, then we may explain the correlation between the position and magnitude of maximum enhancement of  $J_c/J_{c0}$  as a function of the dose. If the migration of a point defect is limited, then we may end up with many but small point-defect pinners, which would result in a peak at lower dose with smaller magnitude of  $J_c/J_{c0}$ . If the migration of point defects is not limited, we may end up with fewer but larger cluster-defect pinners, which results in a peak at higher dose and with higher magnitude.

### C. $T_c$ and annealing studies

Even though limited  $T_c$  measurements were made on our electron-irradiated single crystals, two interesting observations resulted, especially for the annealed crystals *E* and *F*. Both of these observations suggest that oxygen ordering in the chains can be achieved by electron irradiation and annealing, while an increase in  $J_c$  can be produced following the same irradiation and annealing. This argues for a primary pinning defect (for  $\mathbf{H} \parallel c$ ) not associated with oxygen disorder in the chains on a local or unit-cell scale. However, in agreement with preliminary results of a 400-keV electron irradiation,<sup>17</sup> the removal of some extended regions of oxygen deficiency, possible pinning defects, by radiation-enhanced oxygen diffusion appears possible. Creation of such extended regions is unlikely under electron irradiation, since oxygen occupancy in the chains follows ordering, not clustering thermodynamics.

### D. Comparison with protons

A large enhancement in  $J_c$  of Y-Ba-Cu-O crystals in a magnetic field has been observed after irradiation with 3-MeV protons.<sup>3</sup> The authors concluded that the dose

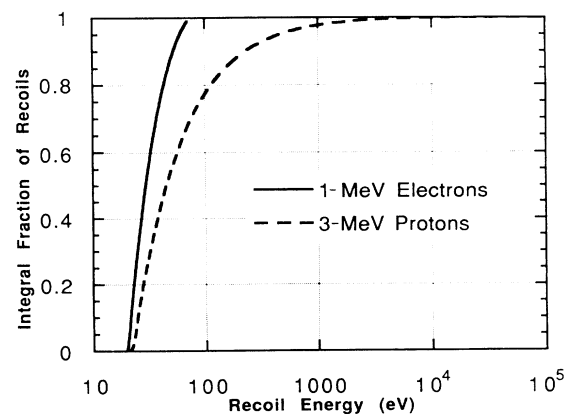


FIG. 9. Integral recoil fraction as a function of recoil energy for 1-MeV electron and 3-MeV proton irradiations.

TABLE II. Comparison of  $J_c$  enhancements due to 2-MeV-electron and 3-MeV-proton irradiation.

Irradiation	$J_{c0}$ (10 K, 2 T) (A cm <sup>-2</sup> )	$J_c^{irrad}$ (10 K, 2 T) (A cm <sup>-2</sup> )	Dose (particles/cm <sup>2</sup> )
1-MeV electrons	$1.64 \times 10^6$	$3.08 \times 10^6$	$1 \times 10^{19}$
3-MeV protons (Ref. 15)	$1.11 \times 10^6$	$7.16 \times 10^6$	$1 \times 10^{16}$

dependence of  $J_c$  suggests that the pinning is dominated by randomly distributed point defects generated by the protons and not by the TEM-visible isolated clusters of defects.

The enhancement of  $J_c$  after low- and room-temperature electron-irradiation damage and TEM results demonstrate unambiguously the pinning of the flux vortices by point defects or small clusters in Y-Ba-Cu-O of sizes  $< 2$  nm. But now the following question is raised by examining Table II: Why does 1-MeV electron irradiation not cause  $J_c$  enhancements comparable to the 3-MeV proton irradiation case?

A possible explanation could be found in the different distributions of recoil energies, as displayed in Fig. 9. The difference in pinning measured at 10 K might be due to the higher-energy recoils not present in electron irradiation, and these higher-energy recoils produce larger defects, such as cascade defects, which can pin more effectively at 10 K than simple point defects or their small clusters.

Another explanation could be that electron irradiation at 1 MeV does not exceed a threshold energy for displacement of one of the heavier-atom species and that an atom defect or its cluster is the stronger pinning defect at 10 K. However, preliminary results from a 2-MeV electron irradiation show an increase in  $J_c$  similar to that at 1 MeV. The maximum recoil energies at 2 MeV of all atoms exceed 90 eV, as shown in Fig. 8, and most likely that is sufficient recoil energy to displace any atom in this material. In view of these results, the former explanation becomes more probable than the latter one.

## V. CONCLUSION

We have shown that 1-MeV electron irradiation results in an enhancement of  $J_c$  in Y-Ba-Cu-O single crystals. Values up to 2 times the preirradiation  $J_c$  at 10 K and 1 T are observed. *In situ* TEM studies in the HVEM suggest that the pinning centers must be small ( $< 2$  nm). We compare our results with those of proton-irradiation experiments and find a lower magnitude of the enhancement of  $J_c$  at 10 K and 2 T. The probable explanation is the difference in the energy spectra of the PKA's produced by the two types of irradiation. The evidence from annealing studies suggests that the primary pinning center produced by electron irradiation is not associated with the oxygen in the chains. Instead, based on our calculations of cross sections for displacement in the four different sublattices, we suggest that the primary pinning defect is most likely the displacement of a copper atom from the CuO<sub>2</sub> plane.

## ACKNOWLEDGMENTS

It is a pleasure to acknowledge helpful and stimulating discussions regarding this work with M. Frischherz, M. Bench, H. Viswanathan, B. Vlcek, and S. Stupp. This research was supported in part by National Science Foundation Grant Nos. DMR 89-20538 (J.G. and D.M.G.), DMR 88-09854 (W.C.L.) through the Science and Technology Center for Superconductivity, and DMR 90-17371 (J.P.R.), and in part by the U.S. Department of Energy BES-Materials Sciences, under Contract No. W-31-109-ENG-38 (M.A.K.).

<sup>1</sup>A. Umezawa, G. W. Crabtree, J. Z. Liu, H. W. Weber, K. W. Kwok, L. H. Nunez, T. J. Moran, and C. H. Sowers, Phys. Rev. B **36**, 7151 (1987).

<sup>2</sup>H. W. Weber, in *Studies of High Temperature Superconductors*, edited by A. V. Narlikar (Nova Science, New York, 1989), Vol. 3, p. 197.

<sup>3</sup>L. Civale, M. W. McElfresh, A. D. Marwick, T. K. Worthington, A. P. Malozemoff, F. H. Holtzberg, C. Field, J. R. Thompson, D. K. Christen, and M. A. Kirk, in Proceedings of the XII Winter Meeting on Low-Temperature Physics, Cuernavaca, Mexico (unpublished).

<sup>4</sup>K. Shiraishi, T. Kato, and J. Kuniya, J. Appl. Phys. **28**, L807 (1989).

<sup>5</sup>M. Konczykowski, Physica A **168**, 291 (1990).

<sup>6</sup>J. P. Rice, B. G. Pazol, D. M. Ginsberg, T. J. Moran, and M. B. Weissman, J. Low Temp. Phys. **72**, 345 (1989).

<sup>7</sup>R. Wheeler, Ultramicroscopy **35**, 59 (1991).

<sup>8</sup>C. P. Bean, Phys. Rev. Lett. **8**, 250 (1962).

<sup>9</sup>E. J. Kramer, J. Nucl. Mater. **72**, 5 (1978).

<sup>10</sup>F. Seitz and J. S. Koehler, in *Solid State Physics*, edited by F. Seitz and D. Turnbull (Academic, New York, 1956), Vol. 2, p. 305.

<sup>11</sup>L. Katz and A. S. Penfold, Rev. Mod. Phys. **24**, 28 (1952).

<sup>12</sup>P. H. Kes, private communication.

<sup>13</sup>H. W. Weber and G. W. Crabtree, in *Studies of High Temperature Superconductors*, edited by A. V. Narlikar (Nova Science, New York, 1991), Vol. 9.

<sup>14</sup>S. T. Secula, J. Nucl. Mater. **72**, 91 (1978).

<sup>15</sup>H. Viswanathan (private communication). The quoted values are the average of four crystals.

<sup>16</sup>U. Welp, W. K. Kwok, G. W. Crabtree, K. G. Vandervoort, and J. Z. Liu, Phys. Rev. Lett. **62**, 1908 (1989).

<sup>17</sup>J. Giapintzakis *et al.* (unpublished).

1.1-MeV Electron Irradiation to  $3 \times 10^{20} \text{ cm}^{-2}$

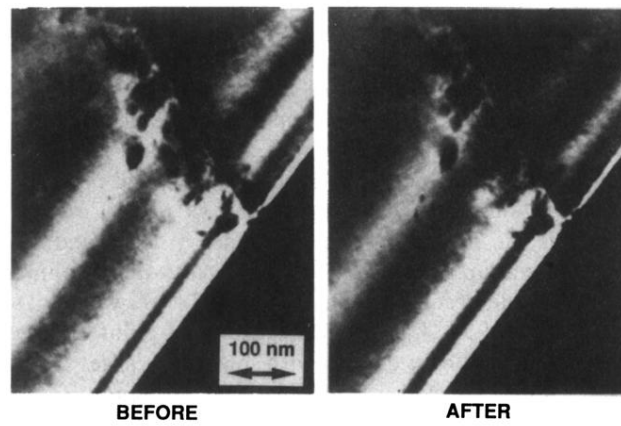


FIG. 7. TEM micrographs of the same region (a) before and (b) after electron irradiation ( $G = 200$  dark field).